Development of Floquet Theory and Applications in Time Crystals

A Thesis

submitted to
Indian Institute of Science Education and Research Pune
in partial fulfilment of the requirements for the
BS-MS Dual Degree Programme

by

Sahil Prabhudesai

Indian Institute of Science Education and Research, Pune
Dr. Homi Bhabha Road,
Pashan, Pune 411008, India.

May, 2024

Supervisor: Dr. Debraj Rakshit

Certificate

This is to certify that this dissertation entitled Development of Floquet Theory and Applications in Time Crystals towards the partial fulfilment of the BS-MS dual degree programme at the Indian Institute of Science Education and Research, Pune represents study/work carried out by Sahil Prabhudesai at the Harishchandra Research Institute(HRI), Prayagraj under the supervision of Dr. Debraj Rakshit, during the academic year 2023-2024.

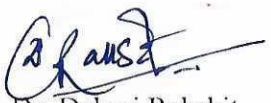

Dr. Debraj Rakshit

Committee:
Dr. Debraj Rakshit

This thesis is dedicated to my parents...

Declaration

I hereby declare that the matter embodied in the report entitled ” Development of Floquet Theory and Applications in Time Crystals ” are the results of the work carried out by me at Harish-Chandra Research Institute (HRI), Prayagraj under the supervision of Dr. Debraj Rakshit and the same has not been submitted elsewhere for any other degree. Wherever others contribute, every effort is made to indicate this clearly, with due reference to the literature and acknowledgement of collaborative research and discussions.

Sahil Prabhudesai
20191139

Acknowledgments

I would like to express my gratitude towards Dr. Debraj Rakshit, my supervisor from the Harish-Chandra Research Institute (Quantum Information and Computation), for giving me this opportunity and for handholding me throughout the complete process of my research. I would like to thank my expert advisor from IISER Pune, Dr. Sreejith G.J., for his guidance. I would also like to thank Ayan Sahoo (a Ph.D. student) and the QIC (Quantum Information and Computation) group of the Harish-Chandra Research Institute (HRI) for their support and guidance during my stay at HRI. I would also like to thank IISER Pune for giving me this opportunity to work on my master's project.

Contents

1 Introduction **7**
1.1 Floquet Theory 7
1.2 Time Crystal 8

2 Implementation of Floquet Technique **13**

3 Floquet driven time crystals under Stark and quasi-periodic modulations **17**
3.1 Stark Many-Body Localization induced time crystal 18
3.2 Time Crystal under quasi-periodic modulation 22
3.3 Prospects of Quasi-periodic time crystal Under controlled rotations of the local Spins 30

4 Conclusion **39**

List of Figures

2.1 Floquet technique:QFI vs time 16

3.1 State averaged-fidelity vs Floquet Cycles 20
3.2 FFT and Energy pairs for Stark Localization 21
3.3 Fidelity and energy pairs for ε=0 24
3.4 Fidelity and energy pairs for ε=0.05 25
3.5 Fidelity and energy pairs for ε=0.1 25
3.6 State averaged-fidelity vs Floquet Cycles for quasi-periodic 28
3.7 Quasi in interaction term 29
3.8 Fidelity fourier transform for $\frac{\pi}{2}$ to $\frac{-\pi}{2}$ with equal divisions 31
3.9 Fidelity fourier transform for $\frac{\pi}{2}$ to $\frac{\pi}{2}$ with equal divisions 32
3.10 Half-wave modulation 33
3.11 Full-wave modulation 34
3.12 Full-wave:State averaged-fidelity vs Floquet Cycles 35
3.13 Dynamics and energy pairs for full-wave modulation 36

List of Tables

3.1 State with cycles 27
3.2 Magnetization with cycles 27
3.3 Magnetization for each spin 28

Abstract

Discrete time crystals are an emerging research topic in quantum many-body physics and condensed matter. The concept of time translational symmetry breaking which governs discrete time crystals is an interesting topic of study. The system under study is the Aubry-Andre-Harper model which has been used along with discrete time crystal to involve some site-dependent quasiperiodicity in the time crystal. The process of Floquet driving is done to evolve the states to different times. Floquet driving technique is a widely used technique to study the dynamics of non-equilibrium systems. In the quasiperiodic time crystal, each spin is given a cosine modulated rotation(full-wave) at each cycle of rotation. When each spin is given the same rotation of π, the initial state repeats after two cycles and thus such a time crystal has time period twice that of the original system. Another protocol, where individual spins of the system is subjected to different but fixed rotations periodically, has been studied. Our initial results with this protocol shows certain signatures for realizing time crystals. However, confirmation of the same will require further studies.

Chapter 1

Introduction

1.1 Floquet Theory

Initially developed by Gaston Floquet in the late nineteenth century within the framework of classical mechanics, floquet theory has interesting applications in a number of fields of physics(most notably condensed matter physics and quantum mechanics). A strong framework for comprehending and influencing the behavior of systems driven periodically is provided by its varied and exciting experimental possibilities. Floquet theory is a crucial tool in many areas of physics and engineering for understanding periodic systems. It offers a strong foundation for understanding how dynamical systems respond to periodic disturbances. Floquet engineered many-body systems have recently gained attention of the research community. There the interests are two-fold: Firstly, novel many-body quantum phenomenon can be realized in such systems, e.g., time crystal, and secondly, they pave the way for future quantum technologies, such as quantum sensing and metrology. Periodically driven systems, with a Hamiltonian as in Eqn. 1.1 (which is a periodic function of time), are known as Floquet quantum systems. Considering the Hamiltonian for the system as follows:

$$H(t) = H(\mathrm{t+T}) \tag{1.1}$$

with time period T.

Floquet theory has exciting and varied experimental potential and can provide a strong framework to comprehend and control the behavior of systems driven periodically. Various experimental prospects in the fields of topological phases of matter, quantum simulation, and light-matter

interactions can be studied via Floquet theory. Ultracold atoms in optical lattices is a key area of story in atomic physics [1, 2, 3]. There is a growing focus on applying a time-periodic external force on optical lattice atoms in order to control their behavior [4]. Some of the experimental observations seen in these field are the observation of the Hofstadter Hamiltonian [5, 6] and the observation of the topological Haldane model [7]. Also tunable gauge potentials have been seen and used artificially[8, 9, 10]. Also, there has been observation of effective ferromagnetic domains. In addition, in shaken optical lattices, there has been development of a roton-maxon dispersion for a BoseEinstein condensate [11] are some of the recent experiments in this rapidly expanding field. These experiments suggest that ultracold atoms in periodically driven optical lattices have great potential for modelling a broad range of condensed-matter systems, including high-energy physics models. This could lead to fresh insights into long-standing unanswered topics. The Floquet formalism is a theoretical tool that is widely employed in this recently developed topic. Researchers who work with atoms and molecules in intense laser beams use Floquet theory. Furthermore, driven optical cosine lattices seem to have great prospects in the field of Floquet engineering for many years in the future [4].

One of main objectives of this project is to numerically implement the Floquet technique. The developed technique is then applied to few-spin systems. In particular, we apply this method in context of time crystal. We discuss the idea behind time crystal and several aspects related to it in the following section.

1.2 Time Crystal

Modern physics revolves around the concept of symmetry and its spontaneous breakdown. Time translation symmetry provides the foundation of both the repetition of patterns and the conservation of energy within a conventional dynamical framework. It is therefore reasonable to wonder whether a closed quantum mechanical system could experience a spontaneous break in time translation symmetry [12]. Time crystals are based on the concept of time translational symmetry breaking, as will be discussed further.

A short-review on time crystal related works: Frank Wilczek [12] first introduced the idea of time crystal. He proposed that if the magnetic flux through interacting bosonic ring is selected appropriately, the ring can transition from a ground state preparation, to a periodic motion over time [12]. A no-go theorem [13, 14], on the other hand, subsequently revealed that such temporal crystalline phase cannot be formed in equilibrium. Also, Sacha [15] initially suggested looking for

time crystal dynamics in systems that are driven regularly [15]. In the Refs. [16, 17], the authors studied many-body systems, further concretized this idea. The system may enter in to a many-body localized (MBL) phase in presence of a strong disorder which, in turn, would prevent the system from absorbing drive heat and reaching to a maximally mixed infinite temperature state. The system can then oscillate in this MBL regime with a period that differs from that of the external drive. In turn it prevents the system from thermalizing to the infinite-temperature state. This phase is referred to as a discrete (or Floquet) time crystal (DTC). Hence it sets it apart from Wilczek's initial idea [18].

DTCs have recently been experimentally realized in a number of physical substrates, e.g., trapped ions [19], spatial crystals of ammonium dihydrogen nitrogen-vacancy centers in diamond [20] and phosphate $NH_4H_2PO_4$ [21, 22]. These systems either had some randomness or they were long-range interacting systems. While DTCs were realized in the MBL phase in [19], there was not enough disorder to reach the MBL regime according to the studies conducted in [20, 21, 22]. A search for DTCs not covered by MBL was started as a result. It has been suggested that driven many-body systems with no disorder, such as quenched two- or higher-dimensional short-range Hamiltonians within a set-up of ultracold atoms with all-to-all interaction between the spins [23, 24] and ultracold atoms bouncing on an oscillating mirror [25], exhibit DTC [18].

Discrete Time Crystal: Time crystals are based on the concept of spontaneous symmetry breaking. The breaking of spatial translational symmetry causes crystal formation [12, 26]. Similarly, the breaking of time-translational symmetry is the cause for formation of time crystals. Time-translational symmetry breaking is happens if an observable of the system is time-dependent in thermal equilibrium. However, a thermal equilibrium state $\rho = e^{-\beta H}$, is doesn't depend on time (as $[\rho, H] = 0$), and hence time-translational symmetry-breaking cannot occur [27].

Thus, one needs to consider alternatives to strict thermal equilibrium. The state ρ maintains all of the symmetries of the Hamiltonian, indicating that symmetry cannot be spontaneously disrupted. The solution to this conundrum is well known for other symmetries: A system with spontaneously broken symmetry can break ergodicity and correspondingly, the time span of the symmetry broken state diverges with increasing system size. Hence, as ρ turns out to be non-physical in the thermodynamic limit. This implies an analogous phenomenon, where time required to reach a stable steady state can be obtained in a finite time for time translation symmetry. The required time for reaching the steady state varies exponentially with system size [27].

We note that non-ergodicity happens at the level of eigenstates in a phase with a spontaneously broken symmetry. This helps to translate these ideas into a more practical concept. An Ising ferromagnet, for instance, has ground states that preserve symmetry and can be written as $|\pm\rangle = \frac{|\uparrow\uparrow\uparrow...\rangle \pm |\downarrow\downarrow\downarrow...\rangle}{\sqrt{2}}$. Unitary time evolution cannot lead a short-range correlated initial quantum state to such long-range correlated cat states in finite time due to prompt decoherence caused by the coupling to the environment. However, the Ising symmetry is broken by the physical combinations of $|\uparrow\uparrow\uparrow ...\rangle$ and $|\downarrow\downarrow\downarrow ...\rangle$ [27].

The different rates of the The states winding of the phases of different quantum states implies that they must be superposed for the occurance of the oscillation during evolution in the Time Translational Symmetry-Breaking (TTSB) scenario. Restating it differently, the two cat states $|\pm\rangle$ requires distinct eigenvalues under the time-evolution operator in a time crystal. This is in contrast to the Ising ferromagnet with degenerate eigenvalues. For the cat states, the time evolution operator U_F has eigenvalues $e^{i\omega_\pm}$. These cat states, although not physical, are invariant under time. Subsequently, a physical state $|\uparrow\uparrow\uparrow ...\rangle$ evolves as $U_F^n |\uparrow\uparrow\uparrow ...\rangle \propto cos(\omega n) |\uparrow\uparrow\uparrow ...\rangle + isin(\omega n) |\downarrow\downarrow\downarrow ...\rangle$, where $\omega = \frac{\omega_+ - \omega_-}{2}$.

The existence of DTC in a variety of disordered Floquet systems has been proven by theoretical and numerical investigations. The first observation of time crystals was that of discrete time crystals (DTC), which are also called floquet time crystals [28, 29]. A DTC occurs in a periodically driven system with certain time period T. There operator A satisfies the condition: $A(t) = A(t + nT)$, where $n > 1$ and $n \in \mathbb{Z}$, which breaks the discrete time translational symmetry [30].

Due to the periodic driving, energy conservation in a floquet system is no longer possible. Therefore, a generic system will eventually absorb the energy from periodic drives and heat up to an unlimited temperature in absence of local conservation constraints. Any local physical observable after a long time is assumed to become featureless due to the thermalization of many-body Floquet systems [31, 32, 33]. Emergent local integrals of motion in the many-body localization (MBL) [34, 35] prevents heat absorption from the external drive. However, in order to examine the behavior of discrete-time crystals, it is necessary to average the observable dynamics over many disorder realization. This limits the effectiveness of discrete-time crystal experimental research and necessitates greater quantum resources [36].

In addition to DTCs stabilized by the MBL phase, another DTC phase, in the form of the prethermal phase, can also exists. In many cases, the Floquet dynamics can be thought to be governed by the effective time-independent prethermal Hamiltonian. Beginning from symmetry-breaking initial states of the prethermal Hamiltonian [37], the Floquet system can show DTC dynamics, and thus producing prethermal DTCs [15, 36].

A state $|\psi\rangle$ is said to have short-ranged correlations for a local operator $\Phi(x)$, if $\langle\psi|\Phi(x)\Phi(x')|\psi\rangle - \langle\psi|\Phi(x)|\psi\rangle\langle\psi|\Phi(x')|\psi\rangle \to 0$ as $|x-x'| \to 0$. Discrete time translational symmetry drives the floquet systems at a frequency of $\Omega = \frac{2\pi}{T}$, where T is time period. $U(t_1,t_2)$ is the time evolution operator from time t_1 to time t_2. TTSB occurs if for every t_1 and every state $|\psi(t_1\rangle$, there exists an operator Φ such that $\langle\psi(t_1+T)|\Phi|\psi(t_1+T)\rangle \neq \langle\psi(t_1)|\Phi|\psi(t_1)\rangle$ where $|\psi(t_1$ +T)$\rangle$ = $U(t_1$ +T, $t_1)|\psi(t_1)\rangle$ [27].

TTSB is realized when the Floquet operator $U_f = U(T,0)$ eigenstates are devoid of short-range correlations. The expected value of some observables in such a system is only invariant for translations by nT for some n $>$ 1, despite the fact that the time evolution is invariant under the discrete time translational symmetry induced by the driving peridicity T. Stated otherwise, the response time of the system is a fraction $\frac{\Omega}{n}$ of the initial driving frequency [27].

Chapter 2

Implementation of Floquet Technique

Theoretical concept behind Floquet dynamics: Floquet theory for time periodic Hamiltonian is analogous to space periodic Hamiltonian, which is what is seen in Bloch theory. Similar to Bloch waves in space, there is a basis for Schrodinger equation solutions that are periodic in time up to a phase. The underlying mathematical concept of floquet theory below has been referred to from Supplemental material of [38].

$$|\psi_\alpha(t)\rangle = e^{-i\mu_\alpha t}|\phi_\alpha(t)\rangle \tag{2.1}$$

The real quantities μ_α represent quasienergies or Floquet exponents and the states $|\phi_\alpha(t)\rangle$ = $|\phi_\alpha(\text{t +T})\rangle$ represent Floquet modes. The states $|\psi_\alpha(t)\rangle$ are referred to as Floquet states.

The time evolution operator, according to Floquet theory, can be written with the help of the floquet modes as follows:

$$\hat{U}(t,0) = \sum_\alpha e^{-i\mu_\alpha t}|\phi_\alpha(t)\rangle\langle\phi_\alpha(0)| \tag{2.2}$$

The time evolution operator, where δt lies between 0 and T(where T is the time period of the Hamiltonian), For some time t=nT + δt, where $n \in \mathbb{N}$ can be written as follows:

$$\hat{U}(t,0) = \hat{U}(\delta t,0)\hat{U}^n(T,0) \tag{2.3}$$

$$\hat{U}(T,0) = \sum_\alpha e^{-i\mu_\alpha T}|\phi_\alpha(0)\rangle\langle\phi_\alpha(0)| \tag{2.4}$$

From this equation, we can conclude that $|\phi_\alpha(0)\rangle$ are the eigenvectors of $\hat{U}(T,0)$ and $e^{-i\mu_\alpha T}$ are the eigenvalues.

Usually, the floquet operator(which is the time-ordered time evolution operator for one time period) is calculated in Floquet systems. It is calculated as follows:

$$\hat{U}(T,0) = \mathscr{T} e^{-i\int_0^T H(t)dt} \tag{2.5}$$

where $\mathscr{T}$ is the time-ordering operator.
On taking discrete time-steps instead of continuous ones, it can be written as:

$$\hat{U}(T,0) = \mathscr{T} e^{-i\Sigma_0^T H(t)dt} \tag{2.6}$$

$$\hat{U}(T,0) = \mathscr{T}\left(\prod_0^T e^{-iH(t)dt}\right) \tag{2.7}$$

The state after multiple cycles of time period for the initial state $|\psi(0)\rangle$ is as follows:

$$|\psi(nT)\rangle = \hat{U}^n(T,0)\,|\psi(0)\rangle \tag{2.8}$$

where n is the number of cycles of the time period, which are called Floquet cycles.

Numerical implementation and proof-of-concept: The above mentioned Floquet theory is required in the main system to go through the cycles of time period of the system. For this Floquet technique needs to be first developed and implemented. Floquet technique has been implemented In order to verify the accuracy of the technique developed. Some results from [39], which consider a periodically driven Ising spin chain with a transverse magnetic field, have been reproduced.

From the above mention Floquet theory, Floquet theory on spin-half Ising chain model system was implemented. The model we are dealing with is Ising spin-half chain model with the Hamiltonian as follows [39]:

$$H = \frac{-J_t}{2}\sum_{j=1}^{N}\sigma_x^j\sigma_x^{j+1} - \frac{(h_0 + h_1\sin(\omega t))}{2}\sum_{j=1}^{N}\sigma_z^j \tag{2.9}$$

where J_t is the exchange coupling constant, h_0 is the DC magnetic field strength. This is a very well studied model in condensed matter physics. For h_1=0 case, this model has two distinct quantum phases: Ferromagnetic Phase and Paramagnetic Phase. The critical point of phase transition occurs at J=h_0. If J> h_0 it is ferromagnetic phase and it is paramagnetic phase when J < h_0. In this model periodic boundary conditions are assumed.

In Eq. 2.9, the parameters are taken as follows: ω=1, h_0=1, h_1=1.5, J_t=1. The fidelity is calculated as follows:

$$Fid = \langle \psi(0) | \psi(t) \rangle \tag{2.10}$$

$$|\psi(t)\rangle = U^n |\psi(0)\rangle \tag{2.11}$$

Here n is the floquet cycle and U is the floquet operator. The floquet operator in this case is:

$$U = \mathscr{T}\left(\prod_{0}^{2\pi}\left(e^{iHdt}e^{-iH_V dt}\right)\right) \tag{2.12}$$

In Eq. 2.12, the exponential terms are multiplied for each time-step from 0 to 2π in a time-ordered fashion. The H_V Hamiltonian is the Hamiltonian in Eq. 2.9 with $h_0 + dh$ in place of h_0, where dh=0.001. To calculate quantum fisher information(QFI), the floquet operator has been calculated as in Eqn. 2.12. QFI is a measure of sensitivity of the system. The quantum fisher information is calculated as [40]:

$$F_Q = 8\frac{(1-Fid)}{dh^2} \tag{2.13}$$

The plots of quantum fisher information(QFI) vs time are in Fig. 2.1(a) and Fig. 2.1(b). Both are the same plots but for different time. The plots are as follows:

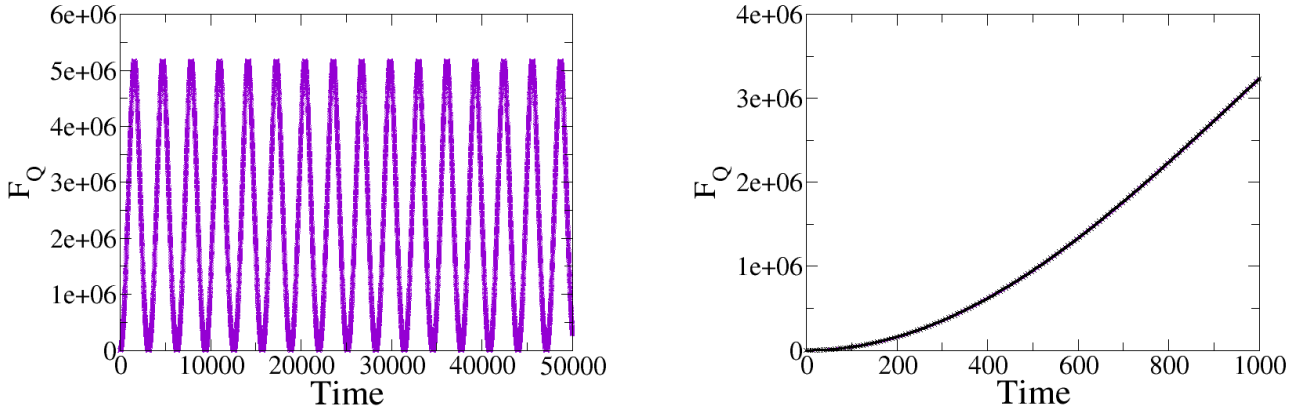

(a) (b)

Figure 2.1: QFI vs time: System size N=6, ω=1, h_0=1, h_1=1.5, J_t=1 in Eq. 2.9 . Time step taken is 0.001. (a) is plot till time=50000 and (b) is plot till time =1000. In (a), the black-line is the plot with time-evolution and purple points are with floquet driving. In (b), the purple line is with time evolution and the purple dots are with floquet driving.

In both these plots, there is a plot of a line and some points. The points plotted, are the values of quantum fisher information at that time which have been obtained via floquet technique described above in this section. These points appear at regular intervals which is the time period of the system which is 2π in this case(as ω=1). The lines which have been plotted is the quantum fisher information obtained without floquet theory by calculating time evolution operator at each step and proceeding with the method.

In both the plots, only one colur is visible as both the lines and points overlap each other. This indicates that floquet theory implemented is in agreement with time evolution operations and is correct. Also the Fig. 2.1(a) has nature similar to "Figure 2(a)" in [39] paper. The quantum fisher information is observed to be periodically repeating and is getting stabilised after some time which is similar in nature to [39].

In [39], they have mentioned that QFI vs time should be of the form x^2 for small time. On fitting Fig. 2.1(b) in gnuplot, QFI $\propto (time)^{1.99}$. So very close to desired result was obtained. Thus floquet technique has been developed and has been used in the system to obtain results over different cycles.

Chapter 3

Floquet driven time crystals under Stark and quasi-periodic modulations

In this chapter, we will apply the developed Floquet technique in the context of Time crystal. Particularly, we shall study Ising spin chain subjected to an additional a) Stark Term, and b) quasi-periodic modulation. A QMB system with short-range interaction enters in to a localized phase in the zero-field limit in presence of a Stark term in the thermodynamic limit, whereas localization happens at a finite strength under quasi-periodically modulation.

As discussed in the introduction, localization is an essential criteria for realizing time crystals in the short-range systems. Although not explicitly proven, certain additional criterion have been identified which are necessary for stable time crystalline nature. We categorically mention them here: i) Time translational symmetry breaking is required for time crystal to exist. In this, for the Hamiltonian H(t+T)=H(t), any observable O(t+T)$\neq$O(t). Rather O(t+nT)=O(t) for some n $>$1. ii)The time crystal should be robust under small perturbations(ε). iii)For the existence of time crystal, observation of energy pairs has been found out to be necessary. The eigen-energies of the floquet Hamiltonian should come in pairs with a fixed energy difference. iv)Presence of some disorder or localization(localization like the quasi term in AAH model) is necessary as a starting driving force to the system. v) Large pool of initial states should satisfy the above conditions, that is, the time crystal behaviour should be followed by most of the initial states. Thus the system should not change irrespective of whichever initial state is chosen.

Now , in the following, we discuss time crystal in the presence of the Stark term.

3.1 Stark Many-Body Localization induced time crystal

This section is a revisit to old work on time crystal on the foundation of which my project is based. This section essentially discusses certain results that have been reproduced from the Ref. [36]. We take a clean floquet Hamiltonian(without strong disorder). This represents a non-trivial Discrete Time crystal phase where any initial state can be taken. Many body localization(MBL) is crucial for stabilizing this inherently dynamical phase. In one-dimensional (1D) systems, quantum systems may enter MBL phases when there is enough random disorder, quasiperiodic potential, or linear Zeeman field. The disorder due to linear Zeeman field is known as Stark MBL. Stark MBL [36] has been used to build a clean many-body Floquet system to stabilize the discrete time crystalline nature. The model considered is as follows [36]:

$$H_1 = \sum_{j=1}^{N} X_j \tag{3.1}$$

$$H_2 = J_z \sum_{j=1}^{N} (j{+}1)\, Z_j Z_{j+1} + W \sum_{j=1}^{N} j Z_j \tag{3.2}$$

$$U_F = e^{-iH_2} e^{-i(\frac{\pi}{2}-\varepsilon)H_1} \tag{3.3}$$

where

$$X = \begin{pmatrix} 0 & 1 \\ 1 & 0 \end{pmatrix}$$

and

$$Z = \begin{pmatrix} 1 & 0 \\ 0 & -1 \end{pmatrix}$$

are the σ_x and σ_z Pauli matrices respectively. The system has periodic boundary conditions.

The H_2 Hamiltonian in Eqn. 3.2, has one linear zz interaction. For stabilizing the discrete time crystal, there is also one linear Zeeman field. This term represents the Stark many-body localization. Both the linear Zeeman field and the Stark MBL are supposed to be suppressed by the perturbation ε . Therefore, in order to stabilize the MBL phase, some nonuniform interaction is required.

The Hamiltonian H_1 in Eqn. 3.1 is the kick or rotation given to the system in each cycle. The ε term represents the imperfection or perturbation given to the system. For the system to be a discrete time crystal, it should robust with perturbation. For ε=0, the term :$e^{-i\left(\frac{\pi}{2}-\varepsilon\right)H_1}$ becomes $e^{-i\left(\frac{\pi}{2}\right)H_1}$. The obtained term denotes rotation about X-axis by angle π and hence the term is responsible for rotation of the spins. This in turn becomes $\Pi_j X_j$.

If $|+z\rangle$ is one of the product state out of the 2^N(N is the system size) product states then $|-z\rangle$=$\Pi_j X_j |+z\rangle$ that is it represents the state with all the spins of $|z\rangle$ flipped. For ε=0, we get "cat states" which are are the quasi-eigenstates of U_F^0 [36].

$$U_F^0 |\pm\rangle = \pm e^{\frac{-i(H_2|z\rangle + H_2|-z\rangle)}{2}} |\pm\rangle \tag{3.4}$$

Here $H_2|+z\rangle$ represents the eigenvalue(energy) that comes when H_2 acts on $|+z\rangle$. Same representation has been used for $|-z\rangle$. The quasi-eigenstates can be written as follows [36]:

$$|\pm\rangle = \frac{1}{\sqrt{2}}\left(e^{\frac{-iH_2|z\rangle}{2}}|z\rangle \pm e^{\frac{-iH_2|-z\rangle}{2}}|-z\rangle\right) \tag{3.5}$$

These $|+\rangle$ and $|-\rangle$ states form a π-pair as the quasi-energy difference between these two states comes as π. If the quasi-energy of the $|+\rangle$ state is denoted as ε_F, then quasi-energy of $|-\rangle$ state will be $\pi - \varepsilon_F$. Product states can be written as a linear combination of the π-pairs as follows[36]:

$$|\pm z\rangle = \frac{1}{\sqrt{2}} e^{\frac{iH_2|\pm z\rangle}{2}} (|+\rangle \pm |-\rangle) \tag{3.6}$$

At ε=0 limit, a trivial subharmonic response is observed as follows [36]:

$$U_F^2 |+z\rangle = U_F |-z\rangle = |+z\rangle \tag{3.7}$$

Physical observables like fidelity or magnetization($\langle m_z(t)\rangle$) repeat after every two cycles for ε=0. Thus their time periods are double of the driving frequency and thus time translation symmetry is breaking. ε=0 is a trivial case. For a non-trivial discrete time crystal $\varepsilon \neq 0$ is taken.

In the paper[36] they have calculated and checked the properties for fidelity as follows:

$$F_n = |\langle\psi_i| U_F^n |\psi_i\rangle|^2 \tag{3.8}$$

here $|\psi_i\rangle$ is the initial state and n is the Floquet cycle.
They have calculated the state averaged fidelity as follows [36]:

$$\overline{F_n} = \frac{1}{2^N}\sum_z |\langle z| U_F^n |z\rangle|^2 \tag{3.9}$$

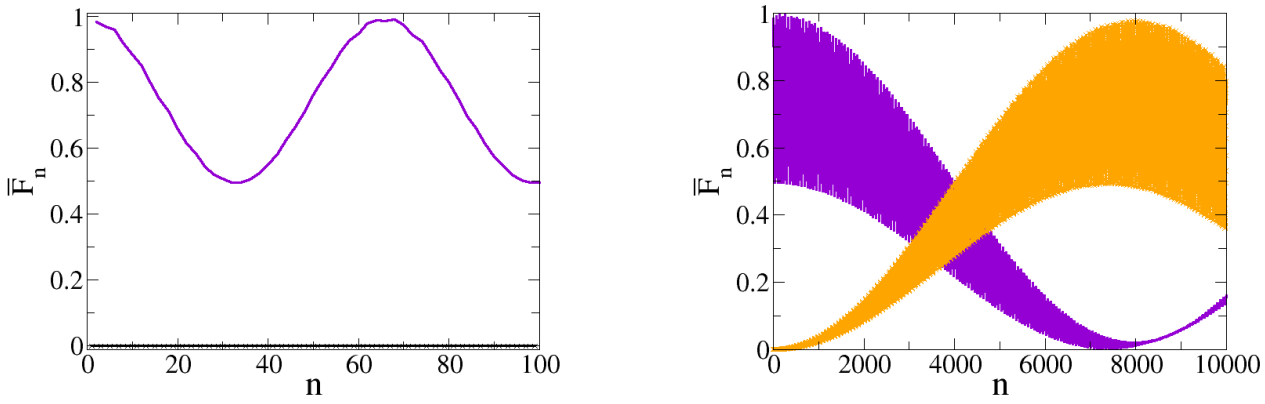

(a) (b)

Figure 3.1: State averaged-fidelity vs Floquet Cycles : System size N=3, J_z=$\frac{\pi}{2N}$=0.52 , W=5, ε=0.05 in Eq. 3.2.(a) is plot of state-averaged fidelity vs floquet cycles for 100 cycles and (b) is plot of state-averaged fidelity vs floquet cycles for 10000 cycles. In (a) the purple line is for even cycles wheras the black line is for odd cycles. In (b), the orange lines are for odd cycles and the purple lines are for even cycles.This is reproduced from [36]

In Figure 3.1(a), the state averaged-fidelity goes from 1 back to 1 and this time period is called the beating time comes as 66 which matches with the paper[36]. Also in 3.1(b) the time period for which the state-averaged fidelity for even cycles goes to from 1 to 0 is another time period which comes as 8000. There is a time period in the paper [36] which is double this , that is 16000 which matches the result here.

Plots of FFT vs ω are made next. This is basically the plot of fast fourier transform of the

fidelity for the state $|1010101\rangle$ vs frequency. Also, I have done plots of overlap vs quasi-energy which are the plots of energy pairs. The eigenenergies of the eigenstates of U_F are the quasi-energies as described above. The $|\pm\rangle$ are the eigenstates of U_F. Overlap is calculated by calculating the fidelity of all the eigenstates of U_F with the initial state as follows:

$$Overlap = |\langle \pm|\psi\rangle|^2 \tag{3.10}$$

where ψ is the initial state.

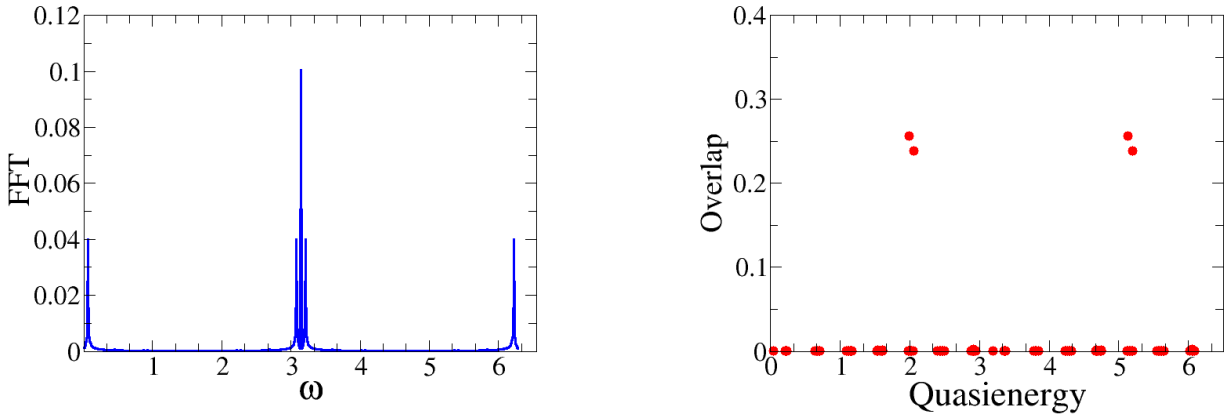

(a) (b)

Figure 3.2: FFT and Energy pairs for Stark Localization: System size N=7, J_z=$\frac{\pi}{2N}$=0.224 , W=5, ε=0.05.(a)Plot of fourier transform of of fidelity vs frequency for the state $|1010101\rangle$ for the Hamiltonian in Eqn. 3.2 and (b) is plot of overlap vs quasienergy for the initial state $|1010101\rangle$ that is the plot of energy pairs

In Fig.3.2(b), it is seen that 2 prominent energy pairs are formed. These energy pairs nave an energy difference close to π. The other states also form energy pairs but are not as prominent as these 2 pairs. From this we can deduce that for, time crystal nature to exist, energy pairs are necessary.

In Fig. 3.2(a), peaks are seen very close to 0, 2π and π. There also smaller peaks at 3.13 and 3.15. The figure shows that the system has become localized to a certain frequency. For attaining time crystal nature, peaks should be attained at only few frequencies. If a lot of peaks are observed at different frequencies, then it is not a time crystal.

Next we will discuss about time crystal with quasi-periodic modulation due to Aubry-Andre-Harper model.

3.2 Time Crystal under quasi-periodic modulation

The main goal of the project is to try the Aubry-Andre-Harper model [41] along with the Discrete Time Crystal and see whether it remains a time crystal and to look at its properties. The AAH model has been implemented in the time crystal by adding quasi-periodic terms in place of interactions.

Localization in Aubry-Andre-Harper: Long-range periodicity intermediate between regular periodic crystals and disordered systems is often shown by aperiodic ordered one-dimensional lattices. Anomalous transport processes in a variety of range of condensed-matter systems, ultracold atoms, photonic, and acoustic systems, among other classical and quantum systems can be investigated via such lattices [41, 42, 43, 44]. Unique properties such as mobility edges, limited modulation of on-site potential showing localization transitions, eigenstates which are multifractal and critical spectra are seen due to quasiperiodicity[41].

The Aubry-Andre-Harper model is an undriven one-dimensional lattice with aperiodic order [45, 46, 47]. The Hamiltonian exhibits a Cantor-set energy spectrum with a phase transition from exponentially confined states(pure point spectrum) to extended states(completely continuous spectrum) as the amplitude of the on-site quasi-periodic potential is decreased below a threshold value, [41, 48].

The localized and delocalized phases are separated by a distinct phase boundary. All the eigenstates transition from exponentially confined to spatially expanded states wen the strength of disorder crosses some threshold value. There may be more intriguing outcomes when the drives become entrenched. Resonantly localized states in the various bands of the AAH model transform and link into extended states with the help of weak space-quasiperiodic and time-periodic drives. On the other hand, the states that do not satisfy the resonant condition stay localized and are not transformed by these drives [49]. It is possible to convert extended states into deep confined states without significant spatial disorder by altering the driving field's amplitude [50, 51, 52, 53, 54].

The fermionic operator representation of the AAH modelis as follows [53, 55, 56]:

$$H = J\sum_{i}\left(\hat{c_{i+1}}^{\dagger}\hat{c}_i + H.c.\right) + V\sum_{i} cos\left(2\pi\omega i\right)\hat{c_i}^{\dagger}\hat{c}_i \tag{3.11}$$

Here V is the potential ω is some irrational number and J is the interaction strength. The operators $\hat{c_i}^{\dagger}$ and $\hat{c}_i$ are the fermionic creation and annhilation operators at the i^{th} site respectively. There is a quasi-periodic term in the system given by the cosine term. The second term of Eq.3.11 is the quasirandom disorder which is the change in on-site energy. This disorder is caused as the potential is incommensurable and is defined by the ratio of the periodicities of the lattice[53, 55, 56].

In the thermodynamic limit, for Eqn. 3.11, phase transition happens at V/J = 2 from delocalized phase to localized phase for almost all irrational lattice periodicity ratio. All single-particle eigenstates are are spatially localized and extended in momentum space wheras the states are spatially expanded and locally confined in momentum space for V/J $<$ 2 [53].

Time crystal with AAH: The model we are dealing with is quasi-periodic time crystal(or time crystal with AAH). The first Hamiltonian H_2 taken is as follows:

$$H_2 = J_z\sum_{j=1}^{N} cos\left(2\pi\omega_2 j\right) Z_j Z_{j+1} + W\sum_{j=1}^{N} cos\left(2\pi\omega_1 j\right) Z_j \tag{3.12}$$

In this Hamiltonian, the goal is to observe the effect of different values of ε on the system and to check whether there are any limitations to its value.

For ε=0:

$$U_F = e^{-iH_2}e^{-i(\frac{\pi}{2})H_1} \tag{3.13}$$

In Fig. 3.3(b), it can be seen that there is only one prominent π energy pair. This satisfies the criteria for time crystal. In Fig. 3.3(a), there is only a single peak which occurs at π. There is no other peak anywhere. The case of ε=0 is a very trivial case. When ε=0, it means no perturbation is given to the spins. Thus it is a trivial case. Due to this reason only a single peak at π is observed in the FFT. For ε=0, the operator U_F has eigenstates which are the "cat states" which can be written as linear combination of 2 oppositely oriented product($|z\rangle$ and $|-z\rangle$) states. Hence it will give just one energy pair.

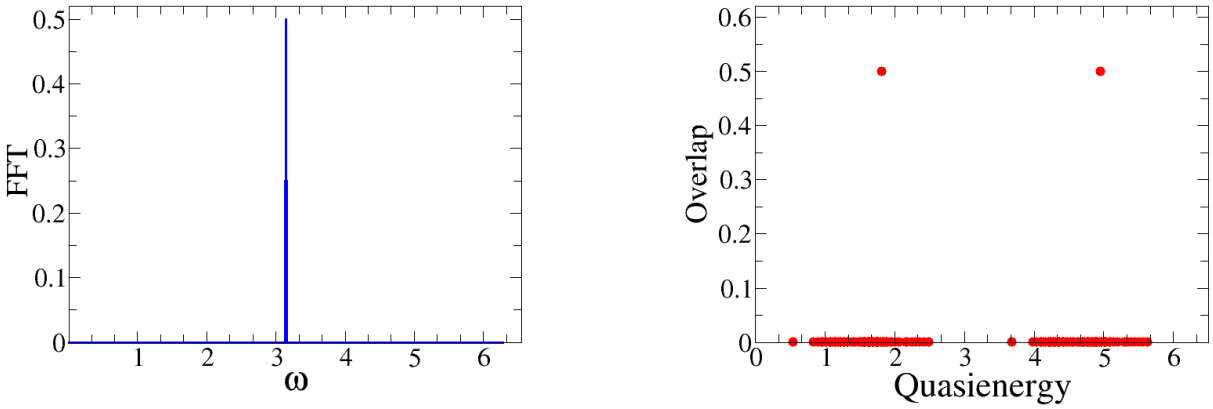

(a) (b)

Figure 3.3: Fidelity and energy pairs for ε=0: System size N=7, J_z=$\frac{\pi}{2N}$=0.224, W=5, ε=0, ω_1=$\frac{\sqrt{5}-1}{2}$, ω_2=$\frac{\sqrt{11}-1}{2}$.(a) The plot is the fourier transform of fidelity vs frequency for the state $|1010101\rangle$ for the Hamiltonian in Eqn. 3.12 (b)Plot of overlap vs quasienergy for the initial state $|1010101\rangle$ that is the plot of energy pairs.

For ε=0.05:

$$U_F = e^{-iH_2} e^{-i(\frac{\pi}{2}-0.05)H_1} \tag{3.14}$$

2 prominent energy pairs each with energy difference π can be observed in Fig.3.4(b). In Fig. 3.4(a), peaks are observed close to 0, π and 2π. Smaller peaks are seen at 3.12 and 3.16. As discussed in Stark localization, this system seems to be localized, having peaks at few frequencies.

When ε=0.05, it means a small perturbation is given to the spins. Thus it is a non-trivial case. Energy pairs exist. Thus it satisfies condition of time crystal. There are peaks at 0, π, 2π and smaller peaks around π. Hence it is a time crystal. For ε=0.05, the eigenstates of the operator U_F can be expressed as some linear combination of some of the product states. Hence it gives more than one energy pair in contrast to ε=0.

For ε=0.1:

$$U_F = e^{-iH_2} e^{-i(\frac{\pi}{2}-0.1)H_1} \tag{3.15}$$

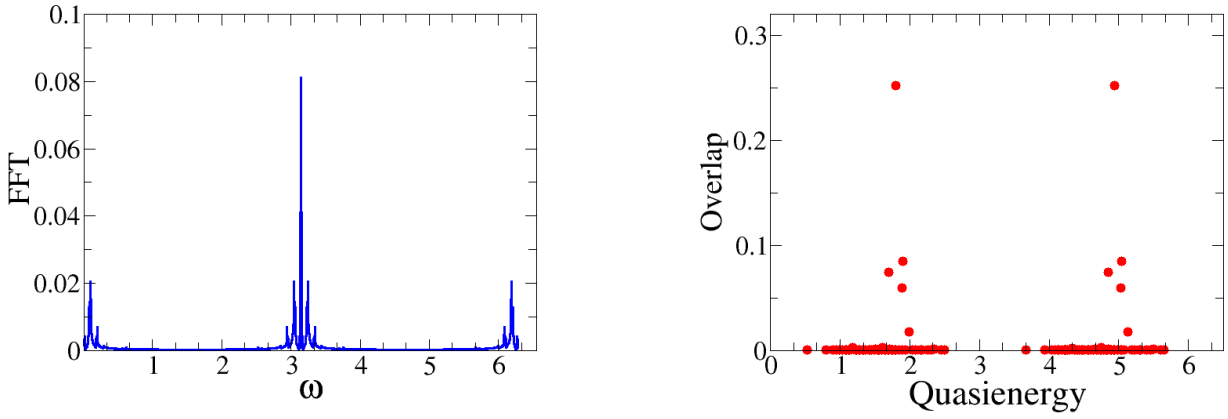

(a) (b)

Figure 3.4: Fidelity and energy pairs for ε=0.05: System size N=7, J_z=$\frac{\pi}{2N}$=0.224 , W=5, ε=0.05, ω_1=$\frac{\sqrt{5}-1}{2}$, ω_2=$\frac{\sqrt{11}-1}{2}$.(a) The plot is the fourier transform of fidelity vs frequency for the state $|1010101\rangle$ for the Hamiltonian in Eqn. 3.12 (b)Plot of overlap vs quasienergy for the initial state $|1010101\rangle$ that is the plot of energy pairs.

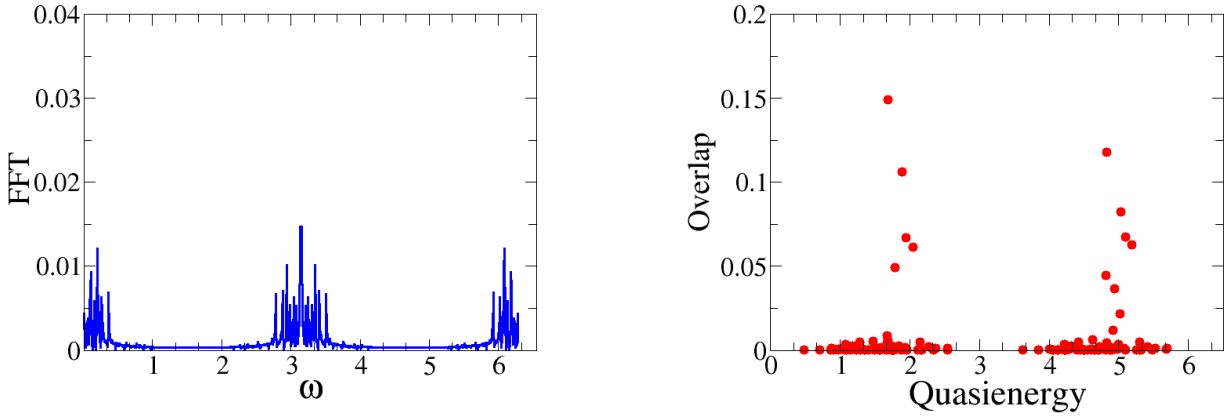

(a) (b)

Figure 3.5: Fidelity and energy pairs for ε=0.1: System size N=7, J_z=$\frac{\pi}{2N}$=0.224, W=5, ε=0.1, ω_1=$\frac{\sqrt{5}-1}{2}$, ω_2=$\frac{\sqrt{11}-1}{2}$.(a) The plot is the fourier transform of fidelity vs frequency for the state $|1010101\rangle$ for the Hamiltonian in Eqn. 3.12 (b)Plot of overlap vs quasienergy for the initial state $|1010101\rangle$ that is the plot of energy pairs.

In Fig. 3.5(b), it can be seen that there is no prominent π energy pair. In this case, π energy

pairs don't exist .This does not satisfy the criteria for time crystal. In Fig. 3.5(a), there are multiple frequencies and hence this phase is not localized and not a time crystal. The time crystal phase has diluted.

When ε=0.1, it is a very large perturbation. Hence the system is unable to maintain its time crystal phase. I have also checked for negative values of ε and it behaves symmetrically that is 0.05 and -0.05 give the same result. This is obvious as perturbation in any direction is symmetric. Also i have checked for values like 0.03 which gives a time crystal phase in between 0 and 0.05. Also for ε=0.5, the time crystal phase is too diltuted with frequencies everywhere and a totally delocalized phase. Thus a small value of ε is necessary. A value close to 0 gives good results. Taking ε=0 gives trivial results. So as to get non-trivial results, ε=0.05 is taken for all cases.

We have seen that quasi-term in both the terms works but we would like to work with quasi-term in only one of the terms if possible to obtain a time crystal for such a system.The next model considered, which is the main focus of our study,is as follows:

$$H_1 = \sum_{j=1}^{N} X_j \tag{3.16}$$

$$H_2 = J_z \sum_{j=1}^{N} cos\,(2\pi\omega j)\, Z_j Z_{j+1} + W \sum_{j=1}^{N} Z_j \tag{3.17}$$

$$U_F = e^{-iH_2} e^{-i(\frac{\pi}{2}-\varepsilon)H_1} \tag{3.18}$$

Here X_j and Z_j are the Pauli matrices at the j^{th} site. Eqn. 3.17 has periodic boundary conditions. The ω term in the H_2 Hamiltonian represents some irrational number.

In this, the term $e^{-i\left(\frac{\pi}{2}-\varepsilon\right)H_1}$ is for rotation of spins. For ε=0, the term :$e^{-i\left(\frac{\pi}{2}-\varepsilon\right)H_1}$ becomes $\Pi_j X_j$. Thus it will only keep flipping the spins every cycle. For example:

Table 3.1: State with cycles

Cycle	**Spin state(for 7spin system)**
Initial state	↓↑↑↑↓↑↓
After 1^{st} cycle	↑↓↓↓↑↓↑
After 2^{nd} cycle	↓↑↑↑↓↑↓
After 3^{rd} cycle	↑↓↓↓↑↓↑
After 4^{th} cycle	↓↑↑↑↓↑↓

This continues with every cycle.Thus the spins come back to their original orientation after every 2 cycles. The same was the case for the Stark localization model in section 3.1. Also I have checked the magnetization (computationally) to verify this. For example for the same state mentioned above, magnetization(measured along Z) m_z is as follows:

Table 3.2: Magnetization with cycles

Cycle	**Spin state(for 7spin system)**	m_z
Initial state	↓↑↑↑↓↑↓	+1
After 1^{st} cycle	↑↓↓↓↑↓↑	-1
After 2^{nd} cycle	↓↑↑↑↓↑↓	+1
After 3^{rd} cycle	↑↓↓↓↑↓↑	-1
After 4^{th} cycle	↓↑↑↑↓↑↓	+1

This continues with every cycle. Thus the system is breaking the discrete time translational symmetry and its repeating its structure after every 2 cycles or 2 time periods. Also π energy pairs exist for all the states. Thus it satisfies requirements for being a time crystal.

The magnetization for each spin for this system under perturbation of ε=0.05 is shown below. In this magnetization is calculated via the pauli Z matrix(m_z).

Table 3.3: Magnetization for each spin

Cycle	1^{st} **Spin**	2^{nd} **Spin**	3^{rd} **Spin**	4^{th} **Spin**	5^{th} **Spin**	6^{th} **Spin**	7^{th} **Spin**
Initial	-1	+1	-1	+1	-1	+1	-1
After 1 cycle	+0.995	-0.995	0,995	-0.995	0.995	-0.995	+0.995
After 2 cycles	-0.998	+0.997	-0.998	+0.999	-0.999	+0.999	-0.997
After 3 cycles	+0.992	-0.992	0.992	-0.992	+0.992	-0.992	+0.992
After 4 cycles	-0.995	+0.988	-0.992	+0.997	-0.998	+0.998	-0.991
After 5 cycles	+0.986	-0.988	+0.986	-0.987	+0.989	-0.989	+0.986
After 6 cycles	-0.989	+0.975	-0.982	+0.993	-0.997	0.997	-0.979

Here, the magnetizations are very close to +1 or -1 and that arises due to the perturbation. In absence of perturbation, it will be either +1 or -1.

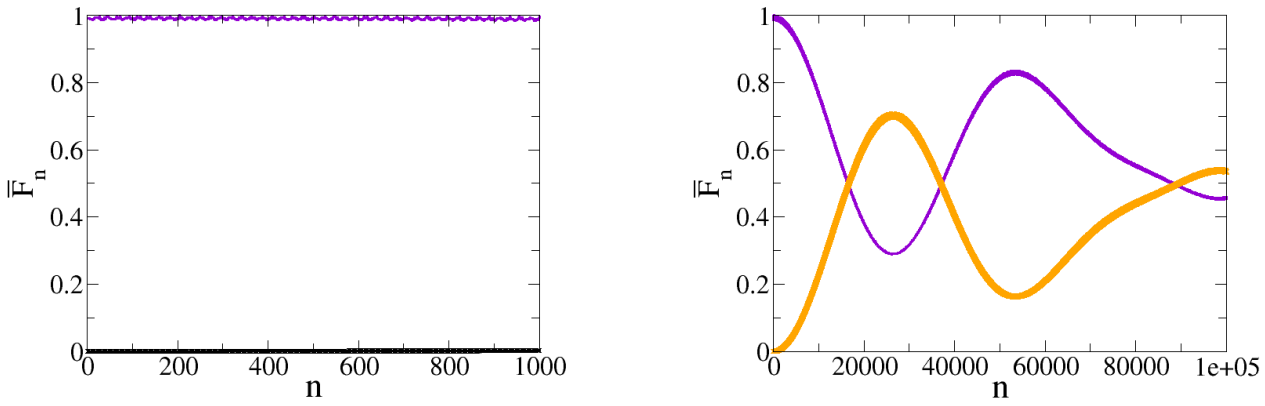

(a) (b)

Figure 3.6: State averaged-fidelity vs Floquet Cycles for quasi-periodic : System size N=3, $J_z=\frac{\pi}{2N}$=0.52 , W=5, ε=0.05 in Eq. 3.19.(a) is plot of state-averaged fidelity vs floquet cycles for 1000 cycles and (b) is plot of state-averaged fidelity vs floquet cycles for 100000 cycles. In (a) the purple line is for even cycles wheras the black line is for odd cycles. In (b), the orange lines are for odd cycles and the purple lines are for even cycles.

In Fig.3.6(a), it can be seen that for even cycles, the values are all 1 and for odd cycles, they are all 0. In Fig.3.6 (b), it can be seen that that both the even and odd cycles start oscillating. But this oscillation is different from that of Stark localization. This is so because of the cosine site dependence of the AAH model.

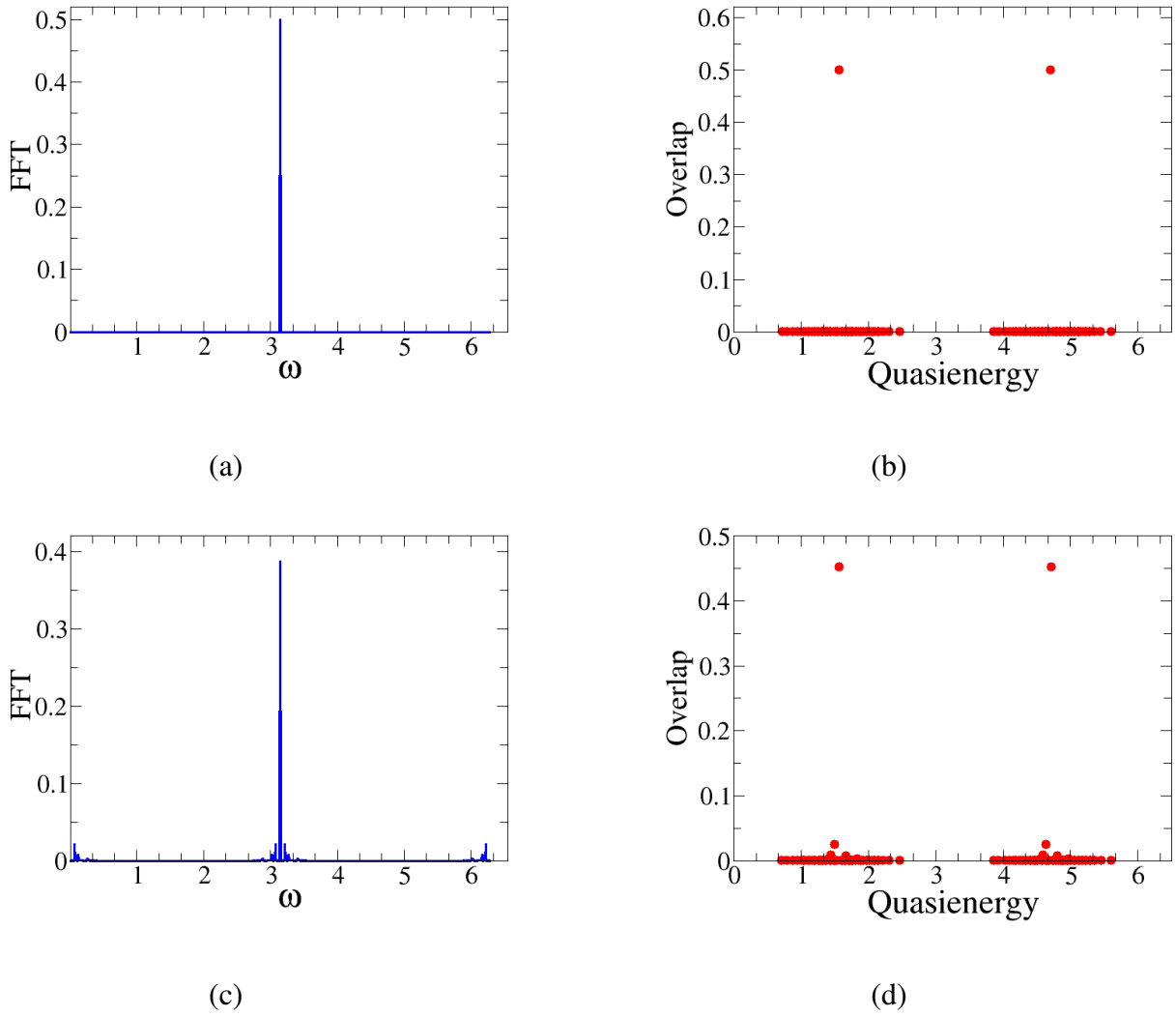

Figure 3.7: Quasi in interaction term: System size N=7, J_z=$\frac{\pi}{2N}$, W=5, ω=$\frac{\sqrt{5}-1}{2}$.(a) The plot is the fourier transform of fidelity vs frequency for the state $|1010101\rangle$ for the Hamiltonian in Eqn. 3.19 for ε=0(b)Plot of overlap vs quasienergy for the initial state $|1010101\rangle$ that is the plot of energy pairs for ε=0. (c) The plot is the fourier transform of fidelity vs frequency for the state $|1010101\rangle$ for the Hamiltonian in Eqn. 3.19 for ε=0.05. (d)Plot of overlap vs quasienergy for the initial state $|1010101\rangle$ that is the plot of energy pairs for ε=0.05.

The Fig.3.7 are the FFT and energy pair plots for Eqn. 3.17 for ε=0 and ε=0.05 in Eqn. 3.18. In Fig. 3.7(a), there is a single peak which occurs at π. Also in Fig. 3.7(b), only one prominent energy pair is seen. Thus this is exhibiting the properties of the trivial case. Also these properties are in accordance with the conditions for time crystal.

In 3.7(c), some small peaks are seen around π , 0 and 2π in addition to the large peak at π. This is due to the small perturbation of ε=0.05. This exhibits very good time crystal nature irrespective of perturbation. Also in 3.7(d), there are 2 prominent energy pairs which satisfies the condition for time crystal.

3.3 Prospects of Quasi-periodic time crystal Under controlled rotations of the local Spins

We explored a new driving protocol, where instead of rotating all the spins by a fixed angle, a controlled rotations of the local spins at specific set of angles has been explored. In the initial case, each spin was given the same rotation angle $\frac{\pi}{2}$ in each cycle. Initially, the U_F operator had the $\frac{\pi}{2}$ term along with H_1, which is responsible for the rotation of each spin. The angle and H_1 is constant for all spins. Hence same rotation is applied to each spin.Instead of this, I have given each spin a different rotation. For this I have done the following cases.

In the first two cases, the angle of rotation has been linearly distributed wheras in the 3^{rd} and 4^{th} case, the angles of rotation have been distributed according to cosine modulation.From previous sections, the Hamiltonian H_2 selected is as follows:

$$H_2 = J_z \sum_{j=1}^{N} cos\,(2\pi\omega j)\, Z_j Z_{j+1} + W \sum_{j=1}^{N} Z_j \tag{3.19}$$

In this section, I have plotted FFT of state-averaged fidelity as in Eqn. 3.9, that is it includes dynamics of all states, to get an idea whether time crystal nature is applicable to all states.

In the previous cases, each spin was given the same rotation angle $\frac{\pi}{2}$ in each cycle. In Eqn. 3.18, the $\frac{\pi}{2}$ term along with H_1 is responsible for the rotation of each spin. The angle and H_1 is constant for all spins. Hence same rotation is applied to each spin. Instead of this, I have given each spin a different rotation. For this I have done the following cases.
Here instead of Eqn. 3.1, the Hamiltonian H_1 becomes as follows:

$$H_1 = \sum_{j=1}^{N} \theta_j X_j \tag{3.20}$$

where θ_j is the angle the j^{th} spin is rotated in every cycle.

Hence U_F becomes:

$$U_F = e^{-iH_2} e^{-iH_1} \tag{3.21}$$

Here, in case of perturbation, that is ε=0.05, θ_j becomes $\theta_j - \varepsilon$.

Case 1:
Giving each spin different rotation starting from $\frac{\pi}{2}$ to -$\frac{\pi}{2}$ with equal divisions of angle between each spin.

In this case, the rotation angle given to each spin is site dependent as follows:

$$\theta_j = \frac{\pi}{2} - \frac{(j-1)\,\pi}{(N-1)} \tag{3.22}$$

where j represents the j^{th} site and N represents the system size.

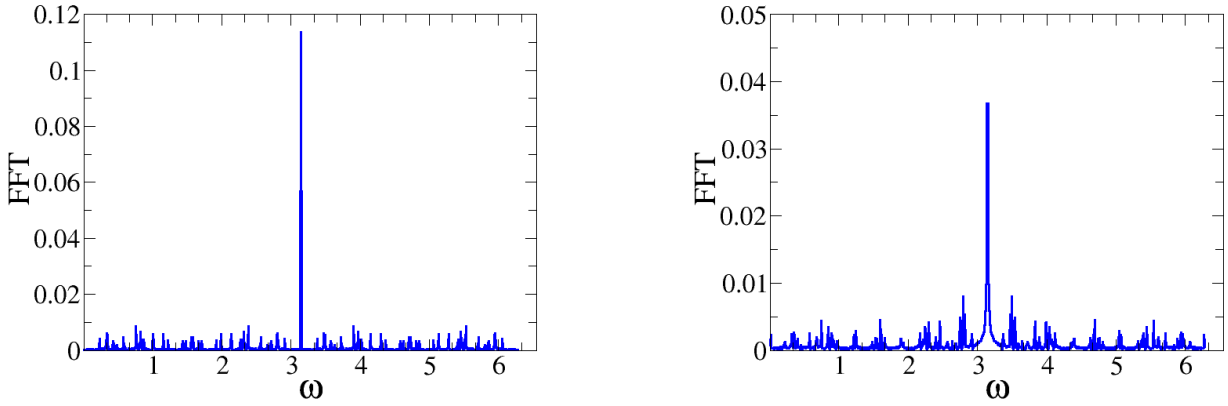

(a) (b)

Figure 3.8: Fidelity fourier transform for $\frac{\pi}{2}$ to $\frac{-\pi}{2}$ with equal divisions: System size N=7, J_z=0.5 , W=1, ε=0.05, ω=$\frac{\sqrt{5}-1}{2}$. The plot is the fourier transform of state-averaged fidelity vs frequency for the Hamiltonian in Eqn. 3.19. (a) is the plot for ε=0 and (b) is the plot for ε=0.05

Figure. 3.8(a), is the plot of when ε=0 and Figure. 3.8(b) is of when ε=0.05. In both these cases, there is a peak at π and some small disturbances at other frequencies. The disturbances

are more for ε=0.05 case as compare to ε=0. The state-averaged-fidelity is showing localization at a single peak(that is at frequency π). Hence most of the states must also be localized at that frequency. Hence this system forms a time crystal.

Case 2: Giving each spin different rotation starting from $\frac{\pi}{2}$ to 0 and back to $\frac{\pi}{2}$ with equal divisions of angle between each spin.
In this case, the rotation angle given to each spin is site dependent as follows:

$$\theta_j = \begin{cases} \frac{\pi}{2} - \frac{(\text{i-1})\pi}{(N\text{-}1)}, & i \leq \frac{\text{N-1}}{2}+1 \\ \\ \frac{(j-1)\pi}{(N\text{-}1)} - \frac{\pi}{2}, & i > \frac{\text{N-1}}{2}+1 \end{cases}$$

where j represents the j^{th} site and N represents the system size.

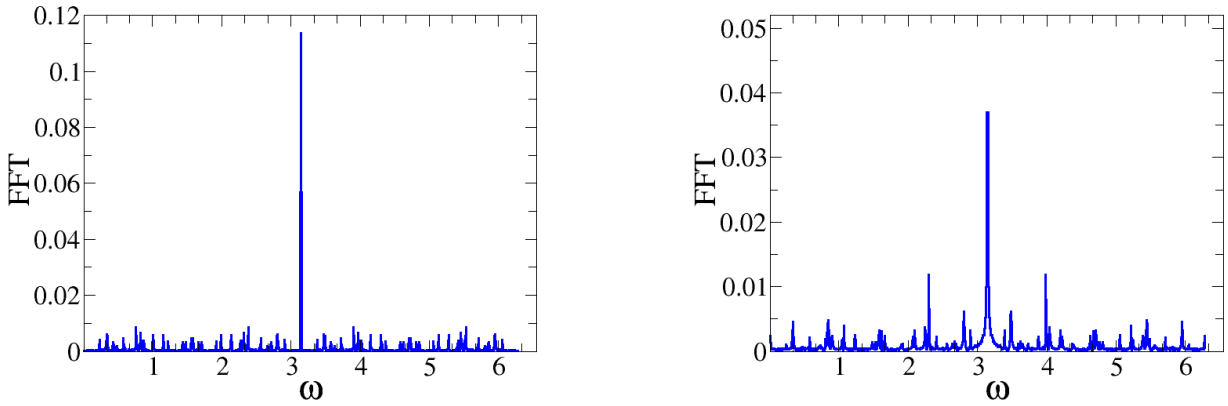

(a) (b)

Figure 3.9: Fidelity fourier transform for $\frac{\pi}{2}$ to $\frac{\pi}{2}$ with equal divisions: System size N=7, J_z=0.5 , W=1, ε=0.05, ω=$\frac{\sqrt{5}-1}{2}$. The plot is the fourier transform of state-averaged fidelity vs frequency for the Hamiltonian in Eqn. 3.19. (a) is the plot for ε=0 and (b) is the plot for ε=0.05

Figure. 3.9(a), is the plot of when ε=0 and Figure. 3.9(b) is of when ε=0.05. In both these cases, there is a peak at π and some small disturbances at other frequencies. The disturbances are more for ε=0.05 case as compare to ε=0. The state-averaged-fidelity is showing localization

at a single peak(that is at frequency π). Hence most of the states must also be localized at that frequency. Hence this system forms a time crystal. This system is giving similar results as that of the first case except that, for the ε=0.05 case, there are more disturbances. this means that this system is more susceptiple and unstable with perturbation.

Case 3: Giving each spin different rotation starting from $\frac{\pi}{2}$ to -$\frac{\pi}{2}$ using cosine modulation (wave modulation) for each spin. This is half wave modulation.
In this case, the rotation angle given to each spin is site dependent as follows:

$$\theta_j = \frac{\pi}{2} cos\left(\pi \frac{(j-1)}{(N\text{-}1)}\right) \tag{3.23}$$

where j represents the j^{th} site and N is the system size.

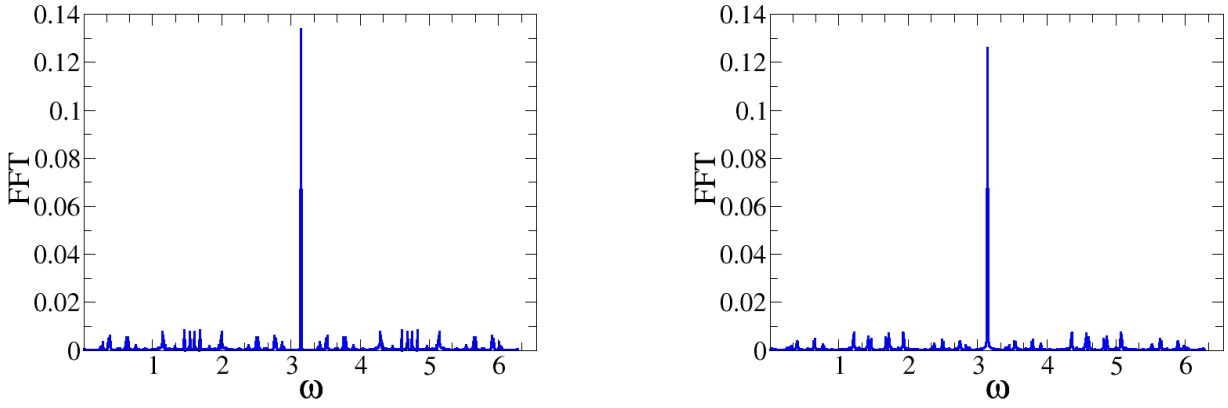

(a) (b)

Figure 3.10: Half-wave modulation: Rotation starting from $\frac{\pi}{2}$ to -$\frac{\pi}{2}$ using cosine modulation. System size N=7, J_z=0.5 , W=1, ε=0.05, ω=$\frac{\sqrt{5}-1}{2}$. The plot is the fourier transform of state-averaged fidelity vs frequency for the Hamiltonian in Eqn. 3.19. (a) is the plot for ε=0 and (b) is the plot for ε=0.05

Figure. 3.10(a), is the plot of when ε=0 and Figure. 3.10(b) is of when ε=0.05. In both these cases, there is a peak at π and some small disturbances at other frequencies. The state-averaged-fidelity is showing localization at a single peak(that is at frequency π). Hence most of the states must also be localized at that frequency. Hence this system forms a time crystal. Here, there isn't much difference between the ε=0 and ε=0.05 case. Thus this system is very stable even with per-

turbation. Also this case is much cleaner than than the first 2 cases as it has lesser disturbances than those cases.

Case 4: Giving each spin different rotation starting from $\frac{\pi}{2}$ to $\frac{\pi}{2}$ using cosine modulation (wave modulation) for each spin. This is full wave modulation.
In this case, the rotation angle given to each spin is site dependent as follows:

$$\theta_j = \frac{\pi}{2} cos\left(2\pi \frac{(j-1)}{(N\text{-}1)}\right) \tag{3.24}$$

where j represents the j^{th} site and N is the system size.

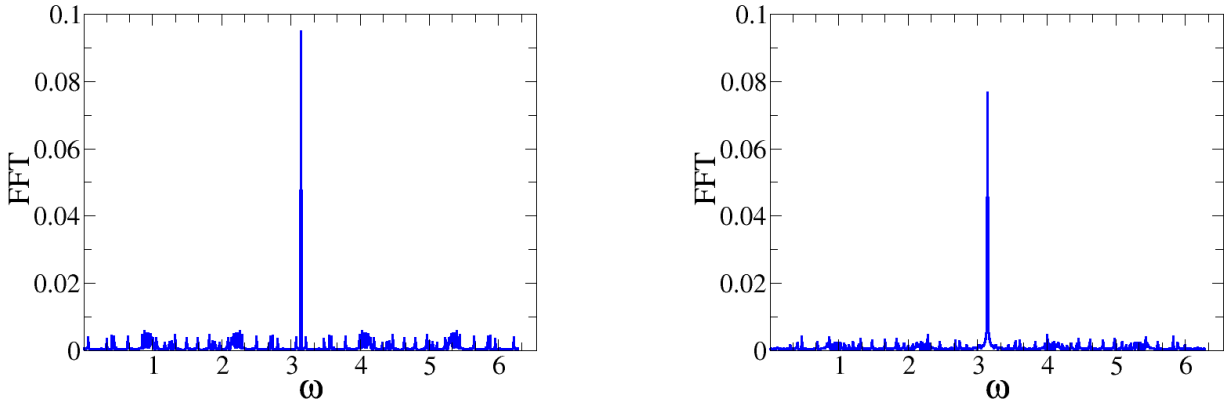

(a) (b)

Figure 3.11: Full-wave modulation: Rotation starting from $\frac{\pi}{2}$ to $\frac{\pi}{2}$ using cosine modulation. System size N=7, J_z=0.5 , W=1, ε=0.05, ω=$\frac{\sqrt{5}-1}{2}$. The plot is the fourier transform of state-averaged fidelity vs frequency for the Hamiltonian in Eqn. 3.19. (a) is the plot for ε=0 and (b) is the plot for ε=0.05

Figure. 3.11(a), is the plot of when ε=0 and Figure. 3.11(b) is of when ε=0.05. In both these cases, there is a peak at π and some small disturbances at other frequencies. The state-averaged-fidelity is showing localization at a single peak(that is at frequency π). Hence most of the states must also be localized at that frequency. Hence this system forms a time crystal. Here, there isn't much difference between the ε=0 and ε=0.05 case. Thus this system is very stable even with perturbation. This case is very similar to Case3 and is much cleaner than than the first 2 cases as it has lesser disturbances than the first 2 cases. The peak at π has lower amplitude here as compared

to Case3.

The main aim is to find time crystal for AAH model and to give each spin a different rotation by cosine modulated rotation to the spin as discussed in Case 3 and Case 4 above. The next section involves the discussion of the dynamics for Case4 , that is full-wave modulation.

Case study for full-wave modulation:Firstly, I have plotted average fidelity vs floquet cycles for the first 200 cyles. I have done this for system size 5. I have taken J_z =0.5 , W=1 and ε=0.05. The plot for this is in Figure 3.12(a). As can be seen in the plot, the state average fidelity for odd cycles is 0 wheras for even cycles it is greater than 0.Figure 3.12(b) is the plot of state averages fidelity vs Floquet cycles for 10000 cycles. I have done this for system size 5. I have taken J_z =0.5 , W=1 and ε=0.05. In this, we can see than as time progresses, the state-averaged fidelity for even Floquet cycles decreases wheras the state-averaged fidelity for odd Floquet cycles increases upto some point and then both start oscillating.

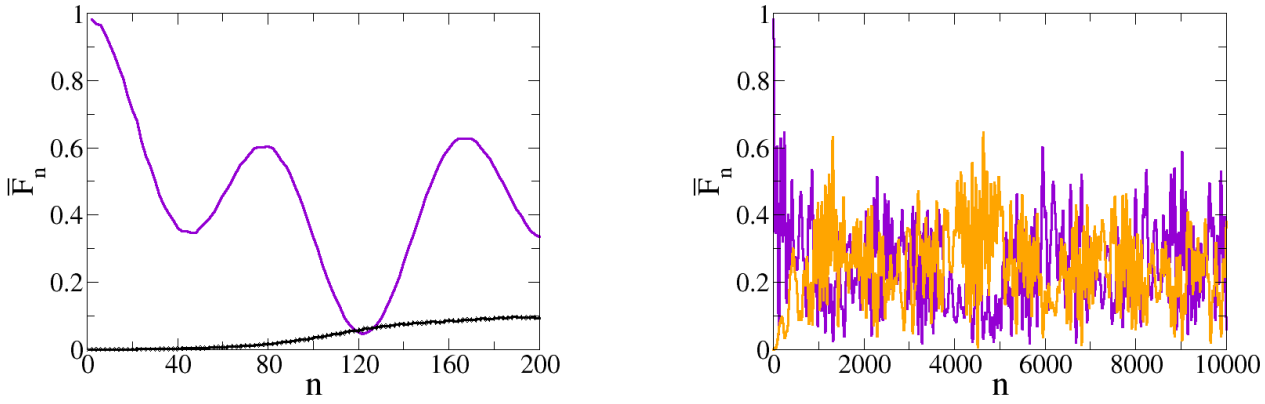

(a) (b)

Figure 3.12: Full-wave:State averaged-fidelity vs Floquet Cycles : System size N=5, J_z=0.5 , W=1, ε=0.05 in Eqn.3.2 for (a) and (b). (a) is plot of state-averaged fidelity vs floquet cycles for 100 cycles and (b) is plot of state-averaged fidelity vs floquet cycles for 10000 cycles.In (a) the purple line is for even cycles wheras the black line is for odd cycles. In (b), the orange lines are for odd cycles and the purple lines are for even cycles.

In Fig 3.12(a) and (b) which are the results of our model, there are no observable time periods. For the 100 cycle plot, the state-averaged fidelity is oscillating but not reaching 1 again. Also in (b) plot, it seems like both the even and odd cycles are stabilising without crossing each other. Thus

there is a chance this model does not form a time crystal.

To verify whether the system forms a time crystal or not, further analysis needs to be done. The analyses that can be done are looking at energy pairs for a large amount of initial states. Also looking into the fidelity of individual states.

Next, analysing the dynamics and the energy pairs for the individual states of the system to confirm whether it surely doesn't exhibit time crystal behaviour.

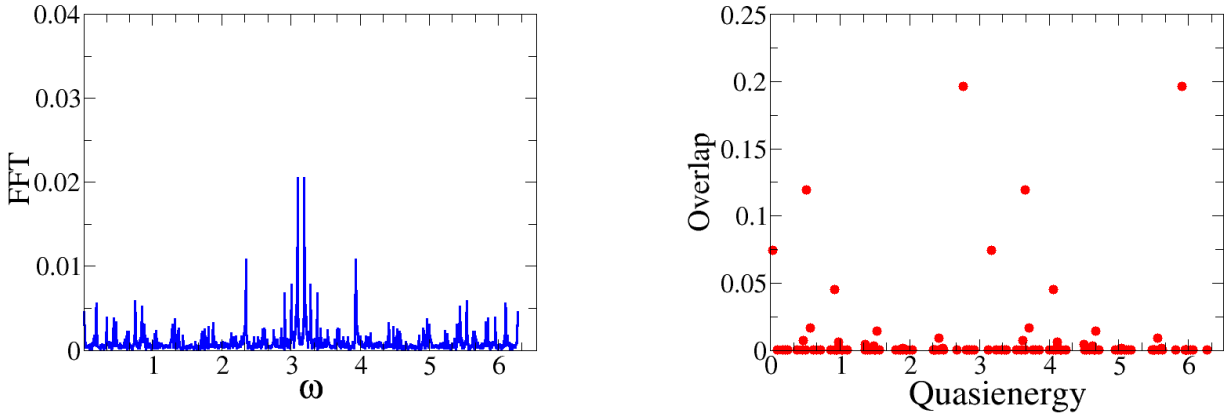

(a) (d)

Figure 3.13: Dynamics and energy pairs for full-wave modulation: System size N=7, J_z=0.5 , W=1, ε=0 in Eqn.3.19 . (a) and (b) are the plot for the state $|1010101\rangle$. (a) is the plot of the fast fourier transform of fidelity vs floquet cycles for the particular initial state. (b) is the energy pair plot for their initial states.

Here 0 represents ↑ and 1 represents ↓ in the intial state.

For both this initial stats, we can see that energy pairs exist. Thus it satisfies condition for time crystal. But for the fourier transform of the fidelity, there are multiple peaks a t various frequencies. Hence the state is not localized at any particuar frequency and this has a lot of disturbances. Hence this does not represent time crystal nature. The presence of energy pairs and multiple frequencies are seen in almost all the states.

It was seen in Fig. 3.11 that the system was localized with few disturbances. We had thus assumed that the system forms a time crystal. The peak at π that occurs in 3.11 is due to the cumulative

peaks at π from all the states. The reason for this peak at π even without time crystal nature needs to be explored further.

Thus our system which is the Hamiltonian in Eqn. 3.19 with each spin having a cosine modulated full-wave rotation cannot be classified as a time crystal. The other kinds of rotation as in Section 3.3 give similar results to full-wave rotation and do not exhibit time crystal nature.

Chapter 4

Conclusion

The project had various goals including developing a few Quantum Many Body(QMB) techniques. The first techniques developed and used were the Exact diagonalization and the Lanczos technique for diagonalizing small or medium size adiabatic QMB systems and their time extensions. The next goal was to implement the techniques for Floquet driving, where a QMB system is periodically disturbed. The other objective was to learn various aspects related to time crystal and to reproduce certain results from the existing literature. One more goal was to realize time crystal in the AAH(Aubry-Andre-Harper) model. In addition, the goal was to design a new protocol within the AAH setup for realizing time crystal. When we provide controlled spin-modulation and implement the protocol there are indications of time crystalline nature although not quite robust.

In the protocol implemented, a time crystal in the AAH model is taken with a full-wave modulated rotation given to the spins. Various models have been tried to obtain a good time crystal with the AAH model. In those trials, it was found that there is a limitation on the value of ε which should not be very large(not greater than 0.05).

In the quasiperiodic time crystal, when each spin is given the same rotation of π, the initial state repeats after two cycles and thus such a time crystal has a time period twice that of the original system. The other protocol, where individual spins of the system are subjected to different but fixed rotations periodically, where each spin is given a cosine modulated rotation(full-wave) at each cycle of rotation has been studied. In this case, certain initial results showed signatures for realizing time crystals. The state-averaged fidelity results for the full-wave modulation showed good results with less disturbance and time crystal behaviour was expected. But for few of the individual state fidelity observed, proper time crystal behaviour was not seen. Thus, further analysis

of more states and further studies need to be done to confirm whether time crystal is obtained or not.

Further works are going on for refining the protocol and remodelling the set-up. The work is going on with higher dimensional spins for realizing time crystal. Also, the efforts are going on for engineering time-crystals where the subharmonic frequencies can be tuned on demand.

Bibliography

[1] Oliver Morsch and Markus Oberthaler. Dynamics of bose-einstein condensates in optical lattices. *Rev. Mod. Phys.*, 78:179–215, Feb 2006.

[2] Immanuel Bloch, Jean Dalibard, and Wilhelm Zwerger. Many-body physics with ultracold gases. *Rev. Mod. Phys.*, 80:885–964, Jul 2008.

[3] Maciej Lewenstein, Anna Sanpera, Veronica Ahufinger, Bogdan Damski, Aditi Sen(De), and Ujjwal Sen. Ultracold atomic gases in optical lattices: mimicking condensed matter physics and beyond. *Advances in Physics*, 56(2):243379, March 2007.

[4] Martin Holthaus. Floquet engineering with quasienergy bands of periodically driven optical lattices. *Journal of Physics B: Atomic, Molecular and Optical Physics*, 49(1):013001, November 2015.

[5] M. Aidelsburger, M. Atala, M. Lohse, J. T. Barreiro, B. Paredes, and I. Bloch. Realization of the hofstadter hamiltonian with ultracold atoms in optical lattices. *Phys. Rev. Lett.*, 111:185301, Oct 2013.

[6] Hirokazu Miyake, Georgios A. Siviloglou, Colin J. Kennedy, William Cody Burton, and Wolfgang Ketterle. Realizing the harper hamiltonian with laser-assisted tunneling in optical lattices. *Phys. Rev. Lett.*, 111:185302, Oct 2013.

[7] Gregor Jotzu, Michael Messer, Rmi Desbuquois, Martin Lebrat, Thomas Uehlinger, Daniel Greif, and Tilman Esslinger. Experimental realization of the topological haldane model with ultracold fermions. *Nature*, 515(7526):237240, November 2014.

[8] J. Struck, C. Ölschläger, M. Weinberg, P. Hauke, J. Simonet, A. Eckardt, M. Lewenstein, K. Sengstock, and P. Windpassinger. Tunable gauge potential for neutral and spinless particles in driven optical lattices. *Phys. Rev. Lett.*, 108:225304, May 2012.

[9] Philipp Hauke, Olivier Tieleman, Alessio Celi, Christoph Ölschläger, Juliette Simonet, Julian Struck, Malte Weinberg, Patrick Windpassinger, Klaus Sengstock, Maciej Lewenstein, and André Eckardt. Non-abelian gauge fields and topological insulators in shaken optical lattices. *Phys. Rev. Lett.*, 109:145301, Oct 2012.

[10] J. Struck, M. Weinberg, C. lschlger, P. Windpassinger, J. Simonet, K. Sengstock, R. Hppner, P. Hauke, A. Eckardt, M. Lewenstein, and L. Mathey. Engineering ising-xy spin-models in a triangular lattice using tunable artificial gauge fields. *Nature Physics*, 9(11):738743, September 2013.

[11] Li-Chung Ha, Logan W. Clark, Colin V. Parker, Brandon M. Anderson, and Cheng Chin. Roton-maxon excitation spectrum of bose condensates in a shaken optical lattice. *Phys. Rev. Lett.*, 114:055301, Feb 2015.

[12] Frank Wilczek. Quantum time crystals. *Physical Review Letters*, 109(16), October 2012.

[13] Patrick Bruno. Impossibility of spontaneously rotating time crystals: A no-go theorem. *Phys. Rev. Lett.*, 111:070402, Aug 2013.

[14] Haruki Watanabe and Masaki Oshikawa. Absence of quantum time crystals. *Phys. Rev. Lett.*, 114:251603, Jun 2015.

[15] Krzysztof Sacha. Modeling spontaneous breaking of time-translation symmetry. *Phys. Rev. A*, 91:033617, Mar 2015.

[16] Vedika Khemani, Achilleas Lazarides, Roderich Moessner, and S. L. Sondhi. Phase structure of driven quantum systems. *Phys. Rev. Lett.*, 116:250401, Jun 2016.

[17] Dominic V. Else, Bela Bauer, and Chetan Nayak. Floquet time crystals. *Phys. Rev. Lett.*, 117:090402, Aug 2016.

[18] Wing Chi Yu, Jirawat Tangpanitanon, Alexander W. Glaetzle, Dieter Jaksch, and Dimitris G. Angelakis. Discrete time crystal in globally driven interacting quantum systems without disorder. *Phys. Rev. A*, 99:033618, Mar 2019.

[19] J. Zhang, P. W. Hess, A. Kyprianidis, P. Becker, A. Lee, J. Smith, G. Pagano, I.-D. Potirniche, A. C. Potter, A. Vishwanath, N. Y. Yao, and C. Monroe. Observation of a discrete time crystal. *Nature*, 543(7644):217220, March 2017.

[20] Soonwon Choi, Joonhee Choi, Renate Landig, Georg Kucsko, Hengyun Zhou, Junichi Isoya, Fedor Jelezko, Shinobu Onoda, Hitoshi Sumiya, Vedika Khemani, Curt von Keyserlingk, Norman Y. Yao, Eugene Demler, and Mikhail D. Lukin. Observation of discrete time-crystalline order in a disordered dipolar many-body system. *Nature*, 543(7644):221225, March 2017.

[21] Jared Rovny, Robert L. Blum, and Sean E. Barrett. Observation of discrete-time-crystal signatures in an ordered dipolar many-body system. *Phys. Rev. Lett.*, 120:180603, May 2018.

[22] Jared Rovny, Robert L. Blum, and Sean E. Barrett. ^{31}P nmr study of discrete time-crystalline signatures in an ordered crystal of ammonium dihydrogen phosphate. *Phys. Rev. B*, 97:184301, May 2018.

[23] Angelo Russomanno, Fernando Iemini, Marcello Dalmonte, and Rosario Fazio. Floquet time crystal in the lipkin-meshkov-glick model. *Phys. Rev. B*, 95:214307, Jun 2017.

[24] Dominic V. Else, Bela Bauer, and Chetan Nayak. Prethermal phases of matter protected by time-translation symmetry. *Phys. Rev. X*, 7:011026, Mar 2017.

[25] Krzysztof Giergiel, Arkadiusz Kosior, Peter Hannaford, and Krzysztof Sacha. Time crystals: Analysis of experimental conditions. *Phys. Rev. A*, 98:013613, Jul 2018.

[26] Alfred Shapere and Frank Wilczek. Classical time crystals. *Phys. Rev. Lett.*, 109:160402, Oct 2012.

[27] Dominic V. Else, Bela Bauer, and Chetan Nayak. Floquet time crystals. *Phys. Rev. Lett.*, 117:090402, Aug 2016.

[28] J. Zhang, P. W. Hess, A. Kyprianidis, P. Becker, A. Lee, J. Smith, G. Pagano, I.-D. Potirniche, A. C. Potter, A. Vishwanath, N. Y. Yao, and C. Monroe. Observation of a discrete time crystal. *Nature*, 543(7644):217220, March 2017.

[29] Soonwon Choi, Joonhee Choi, Renate Landig, Georg Kucsko, Hengyun Zhou, Junichi Isoya, Fedor Jelezko, Shinobu Onoda, Hitoshi Sumiya, Vedika Khemani, Curt von Keyserlingk, Norman Y. Yao, Eugene Demler, and Mikhail D. Lukin. Observation of discrete time-crystalline order in a disordered dipolar many-body system. *Nature*, 543(7644):221225, March 2017.

[30] Fernando Iemini, Rosario Fazio, and Anna Sanpera. Floquet time-crystals as sensors of ac fields, 2023.

[31] Luca D'Alessio and Marcos Rigol. Long-time behavior of isolated periodically driven interacting lattice systems. *Phys. Rev. X*, 4:041048, Dec 2014.

[32] Achilleas Lazarides, Arnab Das, and Roderich Moessner. Equilibrium states of generic quantum systems subject to periodic driving. *Phys. Rev. E*, 90:012110, Jul 2014.

[33] Pedro Ponte, Anushya Chandran, Z. Papi, and Dmitry A. Abanin. Periodically driven ergodic and many-body localized quantum systems. *Annals of Physics*, 353:196–204, 2015.

[34] Maksym Serbyn, Z. Papić, and Dmitry A. Abanin. Local conservation laws and the structure of the many-body localized states. *Phys. Rev. Lett.*, 111:127201, Sep 2013.

[35] David A. Huse, Rahul Nandkishore, and Vadim Oganesyan. Phenomenology of fully many-body-localized systems. *Phys. Rev. B*, 90:174202, Nov 2014.

[36] Shuo Liu, Shi-Xin Zhang, Chang-Yu Hsieh, Shengyu Zhang, and Hong Yao. Discrete time crystal enabled by stark many-body localization. *Phys. Rev. Lett.*, 130:120403, Mar 2023.

[37] Maksym Serbyn, Z. Papić, and Dmitry A. Abanin. Local conservation laws and the structure of the many-body localized states. *Phys. Rev. Lett.*, 111:127201, Sep 2013.

[38] Angelo Russomanno, Alessandro Silva, and Giuseppe E. Santoro. Periodic steady regime and interference in a periodically driven quantum system. *Phys. Rev. Lett.*, 109:257201, Dec 2012.

[39] Utkarsh Mishra and Abolfazl Bayat. Integrable quantum many-body sensors for ac field sensing. *Scientific Reports*, 12(1), August 2022.

[40] Akira Sone, M. Cerezo, Jacob L. Beckey, and Patrick J. Coles. Generalized measure of quantum fisher information. *Phys. Rev. A*, 104:062602, Dec 2021.

[41] Stefano Longhi. Phase transitions in a non-hermitian aubry-andré-harper model. *Phys. Rev. B*, 103:054203, Feb 2021.

[42] Giacomo Roati, Chiara DErrico, Leonardo Fallani, Marco Fattori, Chiara Fort, Matteo Zaccanti, Giovanni Modugno, Michele Modugno, and Massimo Inguscio. Anderson localization of a non-interacting boseeinstein condensate. *Nature*, 453(7197):895898, June 2008.

[43] Bernhard Kramer and Angus MacKinnon. Localization: Theory and experiment. *Rep. Prog. Phys.*, 56:1469–1564, 12 1993.

[44] Y. Lahini, R. Pugatch, F. Pozzi, M. Sorel, R. Morandotti, N. Davidson, and Y. Silberberg. Observation of a localization transition in quasiperiodic photonic lattices. *Phys. Rev. Lett.*, 103:013901, Jun 2009.

[45] P G Harper. Single band motion of conduction electrons in a uniform magnetic field. *Proceedings of the Physical Society. Section A*, 68(10):874, oct 1955.

[46] Serge Aubry and Gilles André. Analyticity breaking and anderson localization in incommensurate lattices. 1980.

[47] Douglas R. Hofstadter. Energy levels and wave functions of bloch electrons in rational and irrational magnetic fields. *Phys. Rev. B*, 14:2239–2249, Sep 1976.

[48] Svetlana Ya. Jitomirskaya. Metal-insulator transition for the almost mathieu operator, 1999.

[49] L. Morales-Molina, E. Doerner, C. Danieli, and S. Flach. Resonant extended states in driven quasiperiodic lattices: Aubry-andre localization by design. *Phys. Rev. A*, 90:043630, Oct 2014.

[50] Klaus Drese and Martin Holthaus. Exploring a metal-insulator transition with ultracold atoms in standing light waves? *Phys. Rev. Lett.*, 78:2932–2935, Apr 1997.

[51] Klaus Drese and Martin Holthaus. Ultracold atoms in modulated standing light waves. *Chemical Physics*, 217(2):201–219, 1997. Dynamics of Driven Quantum Systems.

[52] Eyal Bairey, Gil Refael, and Netanel H. Lindner. Driving induced many-body localization. *Phys. Rev. B*, 96:020201, Jul 2017.

[53] C. M. Dai, W. Wang, and X. X. Yi. Dynamical localization-delocalization crossover in the aubry-andré-harper model. *Phys. Rev. A*, 98:013635, Jul 2018.

[54] P G Harper. The general motion of conduction electrons in a uniform magnetic field, with application to the diamagnetism of metals. *Proceedings of the Physical Society. Section A*, 68(10):879, oct 1955.

[55] Pranjal Bordia, Henrik Lschen, Ulrich Schneider, Michael Knap, and Immanuel Bloch. Periodically driving a many-body localized quantum system. *Nature Physics*, 13(5):460464, January 2017.

[56] Michael Schreiber, Sean S. Hodgman, Pranjal Bordia, Henrik P. Lschen, Mark H. Fischer, Ronen Vosk, Ehud Altman, Ulrich Schneider, and Immanuel Bloch. Observation of many-body localization of interacting fermions in a quasirandom optical lattice. *Science*, 349(6250):842845, August 2015.